Colloids and Surfaces A: Physicochem. Eng. Aspects 444 (2014) 104–113

Contents lists available at ScienceDirect

Colloids and Surfaces A: Physicochemical and Engineering Aspects

journal homepage: www.elsevier.com/locate/colsurfa

Methane adsorption characteristics on coal surface above critical temperature through Dubinin–Astakhov model and Langmuir model

Shixiong Hao[a,b], Wei Chu[a,*], Qian Jiang[a], Xiaopeng Yu[a,b]

[a] Department of Chemical Engineering, Sichuan University, Chengdu 610065, China
[b] Department of Chemical Engineering, Sichuan University of Science & Engineering, Zigong 643000, China

HIGHLIGHTS

- Methods for estimating pseudo-saturation vapor pressure were investigated.
- A procedure of determining the parameter, k, in $p_s = p_c(T/T_c)^k$ was proposed.
- The influence of the characteristic curve form on the prediction was investigated.
- A new form of the characteristic curve was proposed.

GRAPHICAL ABSTRACT

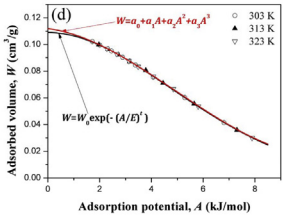

Fig. 5. Characteristiccurvesfor(d) Leiy-1#. The p_s was calculated by the modified Schwarz's method.

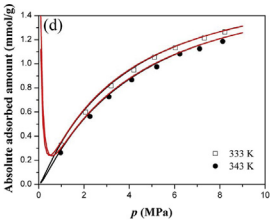

Fig. 6.Experimental *vs* predictive isotherms of methane on: (d) Leiy-1#. The red lines are predictive isotherms which based on Eq. (17) and the black lines are those which based on Eq.(14).

ARTICLE INFO

Article history:
Received 16 October 2013
Received in revised form
11 December 2013
Accepted 24 December 2013
Available online 3 January 2014

Keywords:
Coal
Methane
D–A equation
Pseudo-saturation vapor pressure
Characteristic curve

ABSTRACT

To acquire the required information of the adsorption system under supercritical conditions, four different rank coals were selected as studied samples. The textures of the coals were characterized through N_2 adsorption at 77 K. Their surface morphologies were analyzed by scanning electron microscopy (SEM). The high pressure adsorption data of methane on the coals were obtained at supercritical temperatures. The data were analyzed using the Dubinin–Astakhov (D–A) and Langmuir models. The methods for estimating pseudo-saturation vapor pressure were investigated. And the influence of the characteristic curve form on the D–A equation prediction was investigated. The results show that the constants derived by matching the experimental data to the Langmuir model might lack physical significance, though the Langmuir model was of the correct qualitative form to represent the isotherms of methane on coals. The method for estimating pseudo-saturation vapor pressures proposed by Schwarz failed to render the experimental data to fall onto one characteristic curve. A modified procedure of determining the value of parameter k in Schwarz's equation, i.e. $p_s = p_c(T/T_c)^k$ was proposed. It was found that the modified approach gave the most suitable temperature-independent characteristic curves with determination coefficient $R^2 > 0.9943$. The form of the characteristic curve could influence the D–A model prediction. Using cubic polynomial as characteristic curve form would result in an abnormal prediction i.e. the adsorption amount would increase with the pressure dropping when the pressure is less than approximately 0.9 MPa for Xingq-1–5# and Xujd-1#, 0.8 MPa for Qingh-2–3#, and 0.5 MPa for Leiy-1#. A new form of the characteristic curve deduced from D–A equation was proposed. The prediction uncertainty of D–A equation by using this new characteristic curve form is less than 2.43%.

1. Introduction

Adsorption phenomena are increasingly utilized to perform desired bulk separation or purification purposes [1–5]. Coal is porous material. Coalbed methane (CBM) is unconventional natural gas associated with coal. The key component of CBM is CH_4 (CH_4

* Corresponding author. Tel.: +86 28 85403836; fax: +86 28 85461108.
E-mail address: chuwei1965@scu.edu.cn (W. Chu).

0927-7757/$ – see front matter © 2013 Elsevier B.V. All rights reserved.
http://dx.doi.org/10.1016/j.colsurfa.2013.12.047

content being 88–98% [6]). CBM is retained in coal beds mainly in adsorbed state [7,8]. CBM is not only the major root of coal mine disaster and atmospheric pollution source, but also a valuable non-renewable energy [9]. The interest both in recovery of CH_4 from coal seam and in outburst hazards related to coal mining has led to extensive study of gas sorption in coal [7,9–12].

In recent years, increase in atmospheric CO_2 concentration has raised concern about climate change and led to worldwide efforts on reduction of CO_2 emissions [7,13–18]. Although several options for CO_2 sequestration are being considered, a potentially attractive approach is the storage of CO_2 in deep, unmineable coal beds [7,19]. Such coalbeds frequently contain large amounts of recoverable CH_4, and the recovery of this gas can be enhanced by injecting CO_2 into the coal beds [7,20]. The injection of CO_2 can serve dual purposes to sequester large amounts of CO_2 and to simultaneously provide an increased supply of CH_4. Consequently, some of the sequestration costs can be recovered in the value of the CH_4 produced [7,19].

The design of optimal recovery of CH_4 and CO_2 sequestration in coal beds relies greatly on the availability of high-pressure, supercritical adsorption data for gas sorption as well as reliable adsorption models that are capable of accurate predictions of adsorption phenomena [20]. To simulate reservoir conditions, laboratory sorption experiments are generally conducted at elevated temperature, usually between 293 and 323 K [7,11]. However, the coal bed temperature increases linearly with mining depth increasing [21].

Methane sorption isotherms in coal are commonly IUPAC type I [7]. The Langmuir model is widely used in the CBM industry because of its simplicity and providing a reasonable fit to most experimental data [7]. However, the assumption of an energetically homogeneous surface as proposed by Langmuir theory is not true for coal [11]. Furthermore, the Langmuir model cannot predict methane adsorption amount at different temperatures from one adsorption isotherm. This means that to obtain methane capacity at different temperatures there would be a lot of experiments to do.

The Dubinin–Astakhov (D–A) model has been commonly applied to the description of type I isotherms [22–24]. The D–A equation was mainly developed for the adsorption of vapors below the critical point [22]. However, experiments of gas adsorption on porous solids have shown that there is no abrupt change in the adsorption during the transition from sub-critical to super-critical conditions [22]. This suggests that the D–A equation can be empirically applied to super-critical gases as well [22]. The nice feature of using D–A equation for description of gas adsorption is that a single characteristic curve would be obtained if the characteristic energy is independent of temperature [22]. If the characteristic curve for an adsorption system is known, then adsorption uptake of the adsorbate at different temperatures could be predicted.

The problems of applying the D–A equation to supercritical fluids are [11,22,25]: (1) the estimation of the saturation vapor pressure, p_s. Above the critical temperature, T_c, the concept of saturation vapor pressure does not exist, hence the use of pseudo-saturation vapor pressures was proposed; (2) the density of the adsorbed phase at a given temperature. In order to obtain the volume of adsorbed phase, it is necessary to have a value of adsorbed phase density. The adsorbed phase density is not directly measurable and as a consequence, its value is approximated; and (3) the form of the temperature-invariant characteristic curve to be utilized. The influence of the methods for estimating pseudo-saturation vapor pressures on characteristic curves of activated carbon-methane adsorption systems has been reported [26]. However, to our knowledge, no study has been reported for coal-methane systems, and no study has been reported on the influence of the characteristic curve form on the D–A equation prediction too.

To avoid these problems above, Kim et al. [27] used gas density instead of gas pressure (and adsorbed phase density rather than pseudo-saturation vapor pressure) to modify the classic Dubinin–Radushkevich (D–R) equation, and then applied the modified D–R equation to the gases adsorption on coals under supercritical conditions. However, the modified D–R equation is not convenient to use in CBM industry for the gas density is not as intuitive as pressure.

In the present work, methane adsorption data on four different rank coals were obtained at supercritical temperatures. The D–A equation is applied to methane-coal isotherm data at elevated temperature. The purposes of the current study are: (1) to determine which empirical method presented in the literature to evaluate the pseudo-saturation vapor pressure is most suitable for analyzing the adsorption data above the T_c of methane. The criterion used in our analysis is that the data should be reduced to temperature-independent plots; and (2) to determine the form of the temperature-invariant characteristic curve. The criterion is prediction accuracy.

Table 1
Proximate and ultimate analysis of the coals.

Sample	Proximate analysis wt.%				Ultimate analysis wt.%			
	Ash	VM	FC	Moisture	C	H	O	N
Xingq-1–5#	8.40	29.83	71.17	0.80	77.42	6.58	14.60	1.40
Qingh-2–3#	1.66	21.47	78.53	0.68	84.66	6.47	7.08	1.79
Xujd-1#	11.71	11.66	88.34	0.67	88.70	3.56	4.35	3.39
Leiy-1#	18.45	5.55	94.45	0.15	90.98	1.26	5.53	2.23

Ash was calculated on a dry basis; Volatile matter (VM) and fixed carbon (FC) were calculated on a dried, ash-free basis.

2. Experimental

2.1. Materials

In this work, Xingqing coal (bituminous coal, Qinghai China, labeled as Xingq-1–5#), Qinghua coal (bituminous coal, Qinghai China, labeled as Qingh-2–3#), Xujiadong coal (bituminous coal, Hunan China, labeled as Xujd-1#),and Leiyang coal (anthracite, Hunan China, labeled as Leiy-1#) were used. The proximate analysis and ultimate analysis for the coals are given in Table 1. The oxygen content was determined by difference [28].The sulphur in the four coals was not detected. The coal samples were crushed to particles with size of 60–80 mesh.

2.2. Methods

2.2.1. 2.2.1. Characterization

Textural characterization of the coal samples was conducted using a NOVA1000e surface area and pore size analyzer (Quantachrome Company, USA) with N_2 (at 77 K) as adsorbate. Prior to analysis, samples were degassed at 383 K for 24 h [29]. The specific surface area was calculated by the multipoint BET method [30,31]; the micropore volume was determined by the D-R equation [31,32]; the total pore volume V_t was evaluated from the nitrogen adsorption at $p/p^0 = 0.98–0.99$ [33]; and the pore size distribution was calculated by the by the nonlocal density functional theory (NLDFT) method [31].

Surface morphology was investigated by scanning electron microscopy (SEM) (JEOL/EO JSM-5900, Japan).

2.2.2. Adsorption of methane

The adsorption isotherms were obtained through an equilibrium volumetric method. The detailed experimental method was presented elsewhere [29]. To avoid the influence of water in the coals on the calibration of the reference cell volume, the samples were dried in an oven overnight at 383 K before methane adsorption [29,32].

The precision of the high-precision pressure transducer used in the experiments is 0.05% of the full scale value (maximum pressure 10 MPa). The temperature sensors are Pt 100 Ω RTDs with an estimated uncertainty of 0.1 K. The lines exposed to air were wrapped with heating tape controlled by a PID controller. The purities of the methane and helium used in the experiments are 99.99 and 99.999%, respectively.

2.2.3. Isotherm models

All the conventional isotherm equations were originally derived for absolute adsorption amount ($n_{absolute}$, mmol/g), therefore it should be $n_{absolute}$ to be applied for evaluating the thermodynamic property of adsorbed phase [34]. However, the $n_{absolute}$ that revealing the true mass confined in the adsorbed phase cannot be directly measured. The so-called excess adsorption amount (n_{excess}, mmol/g) that is approached from the experimental equilibrium data is used for the calculation of $n_{absolute}$ [27,29,31]:

$$n_{adsolute} = \frac{n_{excess}}{1 - \rho_{gas}/\rho_{adsorbed}} \quad (1)$$

where ρ_{gas} and $\rho_{adsorbed}$ are the density of the free gas phase and the adsorbed phase, respectively (in g/cm^3).

A major problem in determining absolute sorption is that $\rho_{adsorbed}$ cannot be determined directly and certain assumptions have to be made. Saha et al. [35] proposed a new method to account for the adsorbed phase volume. In this work, we use the Saha's method to calculate the density of the adsorbed phase ($\rho_{adsorbed}$). The Saha's method is as follows [35],

$$\rho_{adsorbed} = \rho_b \exp[-\alpha(T - T_b)] \quad (2)$$

where ρ_b is the density of the liquid methane at the normal boiling point (0.4224 g/cm^3); T_b is normal boiling point of methane (111.67 K); and α is the thermal expansion coefficient of the adsorbed phase that can be expressed as follows [31,35,36].

$$\alpha = \frac{1}{v_{adsorbed}}\left(\frac{\partial v_{adsorbed}}{\partial T}\right) \approx \frac{1}{T} \quad (3)$$

where $\upsilon_{adsorbed}$ is the adsorbed phase specific volume.

2.2.3.1. Langmuir model. The form of the Langmuir equation used herein is expressed as [22]:

$$\frac{n_{absolute}}{n_0} = \frac{bp}{1 + bp} \quad (4)$$

where n_0 is the limiting adsorption capacity (in mmol/g); p is the equilibrium pressure (absolute pressure in MPa); b is the Langmuir constant (in MPa^{-1}). n_0 and b are the adsorption parameters that are optimized from the least-squares criteria using the experimental data.

2.2.3.2. Dubinin–Astakhov (D–A) model. The D–A model for adsorption of methane onto non homogeneous carbonaceous solids is expressed as [22,31]:

$$\frac{W}{W_0} = \exp\left[-\left(\frac{A}{E}\right)^t\right] \quad (5)$$

$$W = \frac{n_{absolute} \times 10^{-3} \times M_{CH_4}}{\rho_{adsorbed}} \quad (6)$$

$$A = RT \ln\frac{p_s}{p} \quad (7)$$

where W is the volume of adsorbed phase at equilibrium (in cm^3/g); W_0 is the limiting volume that the gas can occupy in the adsorbent (in cm^3/g); A is the adsorption potential (in J/mol); E is the characteristic energy of the adsorption system (in J/mol); M_{CH_4} is the molar mass of methane (in g/mol); R is the gas constant; and t is the structural heterogeneity parameter.

In order to calculate the adsorption potential A, the value of the vapor pressure p_s at a given temperature should be known. Saturation vapor pressures are used for adsorbates when temperatures are below T_c [22]. However, above T_c, there is no concept of the vapor pressure; hence the use of pseudo-saturation vapor pressures was proposed. In this study, we use three approaches that existed in the literatures to evaluate the pseudo-saturation vapor pressure above T_c [11,22,26]:

(1) Use Antoine equation for the saturation vapor pressure and extrapolate it to temperatures above the critical temperature [22,26]:

$$\ln p_s = B - \frac{C}{D + T} \quad (8)$$

where B, C, and D are Antoine parameters.

(2) Use the Dubinin's method [11,22]:

$$p_s = p_c\left(\frac{T}{T_c}\right)^2 \quad (9)$$

where the subscript c refers to the critical point (for methane, p_c is 4.5992 MPa, and T_c is 190.56 K).

(3) Use the Amankwah and Schwarz method [22,26]:

$$p_s = p_c\left(\frac{T}{T_c}\right)^k \quad (10)$$

where k is a parameter specific to the adsorbate–adsorbent system.

Table 2
Textural characteristics of the coals.

Sample	S_{BET} (m^2/g)	V_{mic} (mm^3/g)	V_t (mm^3/g)
Xingq-1–5#	2.581	0.4464	4.403
Qingh-2–3#	2.455	0.3723	3.177
Xujd-1#	2.635	0.5143	3.850
Leiy-1#	7.486	3.1190	13.770

3. Results and discussion

3.1. Textural characterization

Table 2 summarizes the textural parameters calculated from the nitrogen isotherms. The pore size distributions are presented in Fig. S2. From Fig. S2, it can be observed that the Xingq-1–5#, Qingh-2–3#, and Xujd-1# have similar pore size distribution. However, the pore size distribution of the Leiy-1# is significantly different from the others.

Fig. S1 shows the SEM images of the typical coal samples. It was observed that the surface morphology of Leiy-1# shows a little different from the Xujd-1#. The particles of Leiy-1# are smaller and arrange more tightly than those of the Xujd-1#. The difference in the surface morphology is in agreement with the S_{BET} and V_{mic} data of coals. If the particles are smaller and arrange more tightly, the S_{BET} or V_{mic} of coal will be higher.

3.2. Langmuir correlations

Fig. 1 shows the methane uptake data measured at 303, 313, and 323 K for the samples. The solid lines in Fig. 1 are Langmuir fit curves. The regressed adsorption parameters (n_0 and b) are listed in Table 3.

According to the assumptions of the Langmuir model, the saturation capacity n_o is supposed to represent a fixed number of

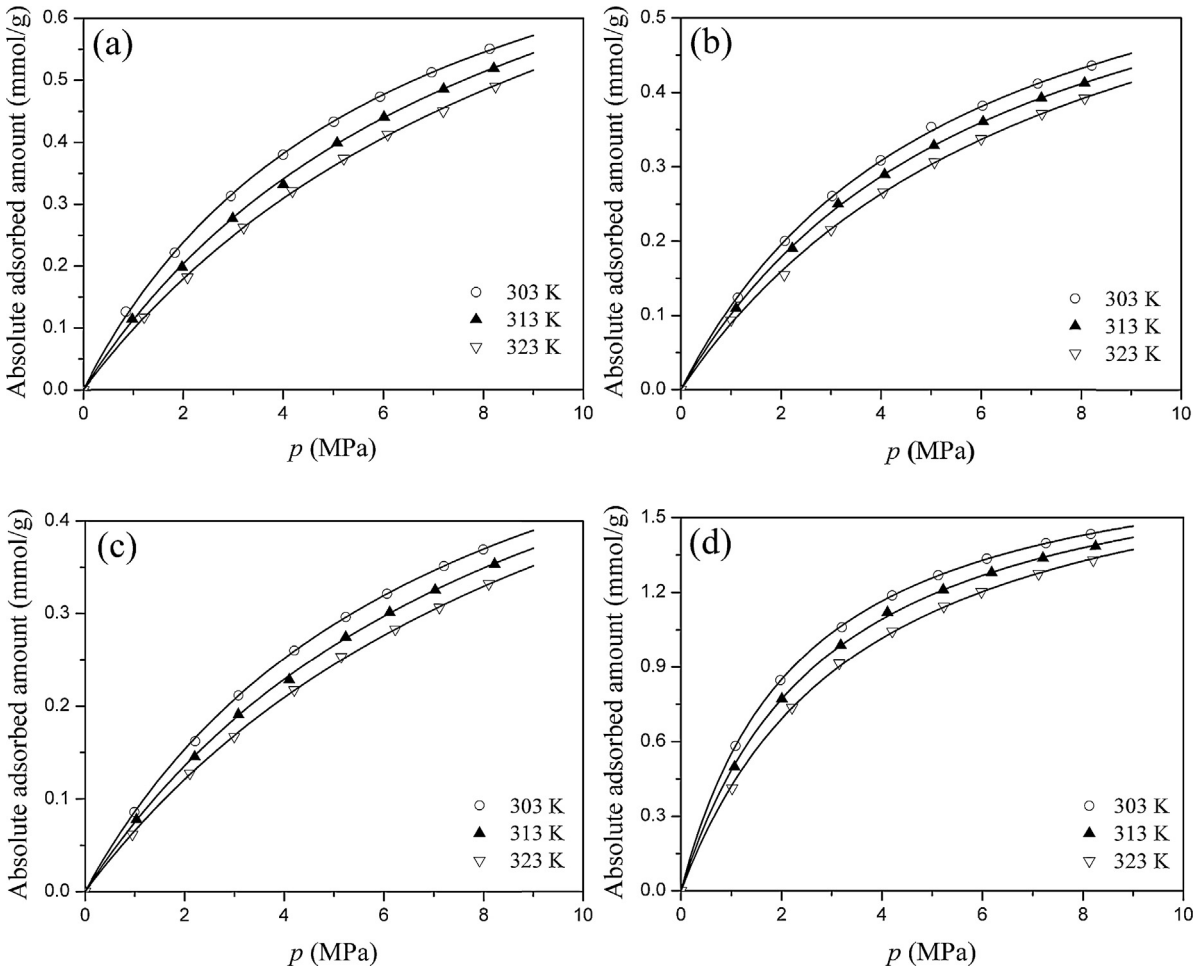

Fig. 1. Langmuir curve fits to methane isotherm data for samples: (a) Xingq-1–5#; (b) Qingh-2–3#; (c) Xujd-1#; and (d) Leiy-1#. Solid lines are curve fits.

surface adsorption site. It should therefore be a temperature-independent constant [37]. However, as shown in Table 3, the saturation capacity n_o is a function of temperature. Similar observations were made by Zhou and Zhou [38] and Clarkson et al. [11]. Ruthven [37] held that the constants derived by matching the experimental data to the Langmuir model might lack physical significance, though the Langmuir model was of the correct qualitative form to represent a type I isotherm. Saturation capacity n_o being a function of temperature in Zhou and Zhou's, Clarkson et al.'s and our studies confirm Ruthven's view.

Table 3
Adsorption parameters of the Langmuir model for adsorption isotherms of methane on the coals at 303, 313, and 323 K.

Sample	T (K)	n_o (mmol/g)	b (MPa^{-1})	R^2
Xingq-1–5#	303	0.9548	0.1663	0.9948
	313	1.0407	0.1217	0.9947
	323	1.1149	0.0959	0.9949
Qingh-2–3#	303	0.7247	0.1848	0.9950
	313	0.7278	0.1628	0.9948
	323	0.7596	0.1327	0.9947
Xujd-1#	303	0.6980	0.1408	0.9951
	313	0.7358	0.1130	0.9949
	323	0.7748	0.0925	0.9949
Leiy-1#	303	1.8489	0.4257	0.9949
	313	1.8711	0.3504	0.9948
	323	1.9093	0.2838	0.9947

3.3. Determination of characteristic curves

3.3.1. Extrapolation Antoine equation method

The Antoine parameters B, C, and D in Eq. (8) were obtained from regression analysis of methane saturation vapor pressure data below T_c. The methane saturation vapor pressure p_s at a given temperature T (range from 100 to 190 K) were obtained from the NIST website [39]. The relationship between T and p_s for methane is shown in Fig. S3. The dot lines in Fig. S3 is the Antoine equation fitting curve. The regressed adsorption parameters (B, C, and D) are 7.7437, 1306.5485, and 19.4362, respectively.

In order to utilize the D–A equation, its three parameters (W_0, E, and t) were evaluated by a non-linear regression procedure. The input data for the regression were the volume of adsorbed phase, W, and the adsorption potential, A.

Fig. 2 shows the characteristic plots for the coals. The volume of adsorbed phase W was calculated by Eq. (6). The adsorption potential A was calculated by Eq. (7), in which the pseudo-saturation vapor pressure p_s was calculated by extrapolation of Antoine equation.

The form of the temperature-invariant characteristic curve to be utilized is one of the important problems associated with the application of potential theories [11]. Amankwah and Schwarz [26], and Clarkson et al. [11] did not give the form of the characteristic curve in their works. Li et al. [40], Su et al. [41] and Feng et al. [42] used polynomial to express the characteristic curve. Although this method is simple, the quadratic or cubic polynomial parameters are lack of physical meaning. In the present work, we deduced an

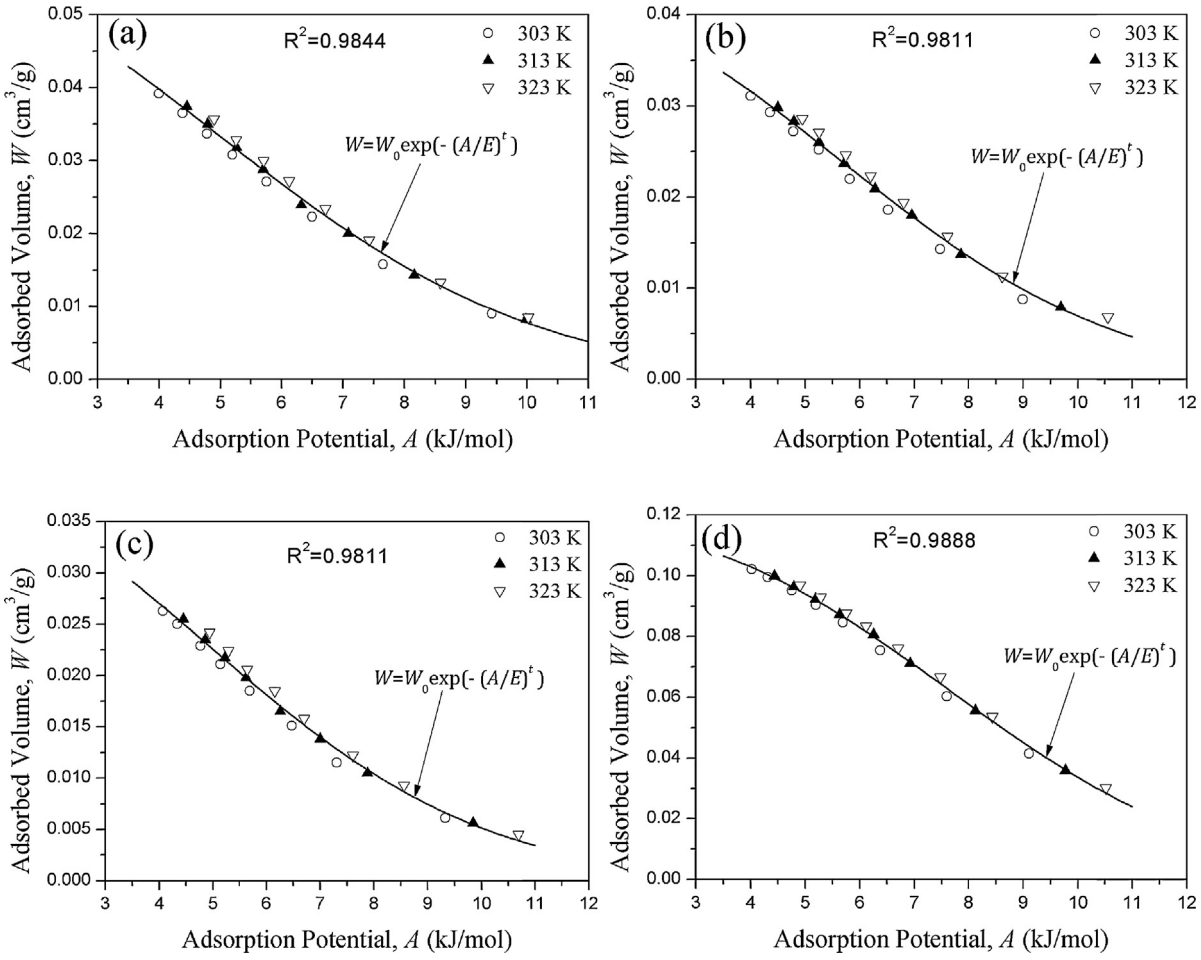

Fig. 2. Characteristic curves for methane on (a) Xingq-1–5#, (b) Qingh-2–3#, (c) Xujd-1#, and (d) Leiy-1#. The p_s was calculated by extrapolation of Antoine's equation.

equation i.e. Eq. (11) from the D–A equation to express the characteristic curve.

$$W = W_0 \exp\left[-\left(\frac{A}{E}\right)^t\right] \tag{11}$$

where W_0, E, and t are parameters to be determined by regression analysis. The input data for the regression analysis were W, and A.

The regressed adsorption parameters (W_0, E, and t) are reported in Table S1. The solid lines in Fig. 2 represent are the characteristic curves calculated from the Eq. (11) using the regressed adsorption parameters (W_0, E, and t). Agarwal and Schwarz [43] defined the maximum deviation of adsorbed phase volume at a particular value of A divided by the maximum adsorption volume ($\times 100$) as deviation. However, there are scarcely two discrete data points of which the A values are same. Consequently, the deviation of adsorbed volume at a particular value of A is not easy to determine accurately. In this paper, we use the determination coefficient, R^2, to indicate the deviation of the data. Obviously, the closer to one the value of R^2, the less discrete the data. The maximum of R^2 is 0.9888 for Leiy-1#, while the minimum of R^2 is 0.9811 for Qingh-2–3# and Xujd-1#s.

3.3.2. Dubinin's method

Extrapolation Antoine equation results in high p_s which are 40.1840 MPa for 303.15 K, 45.3881 MPa for 313.15 K, and 50.9029 MPa for 323.15 K respectively. Flood [43] has proposed that in the absence of any direct experimental information on the adsorbed phase, estimation of p_s as the vapor pressure should be considered empirical. Dubinin's empirical method i.e. Eq. (9) was widely used to calculate the pseudo-saturation vapor pressure in gas-solid adsorption system [26,31,36,44,45].

Fig. 3 shows the characteristic plots for the coals. The solid lines in Fig. 3 represent the characteristic curves calculated from the Eq. (11) using the regressed adsorption parameters (W_0, E, and t) that are listed in Table S2. The pseudo-saturation vapor pressure p_s was calculated by Eq. (9). The maximum of R^2 is 0.9936 for Xujd-1#, while the minimum of R^2 is 0.9920 for Xingq-1–5#. This indicates that characteristic curves using the Dubinin method for pseudo-saturation vapor pressure display smaller deviations than the Antoine equation extrapolation techniques (see Fig. S3).

3.3.3. Schwarz's method

The interaction between an adsorbate and a particular adsorbent would be unique to the adsorption system studied. Amankwah and Schwarz [26] proposed Eq. (10) to estimate pseudo-saturation vapor pressures in application of the D–A equation. To calculate the adsorption potential, A, the value of k in Eq. (10) should be known. However, the value of k is not known a priori. Amankwah and Schwarz [26] used the following method to determine the value of k. When Eq. (10) is used in conjunction with Eq. (5) (i.e. D–A equation), a four parameter equation is obtained:

$$\frac{W}{W_0} = \exp\left[-\left(\frac{\mathrm{RT}}{E}\ln\frac{p_c\left(T/T_c\right)^k}{p}\right)^t\right] \tag{12}$$

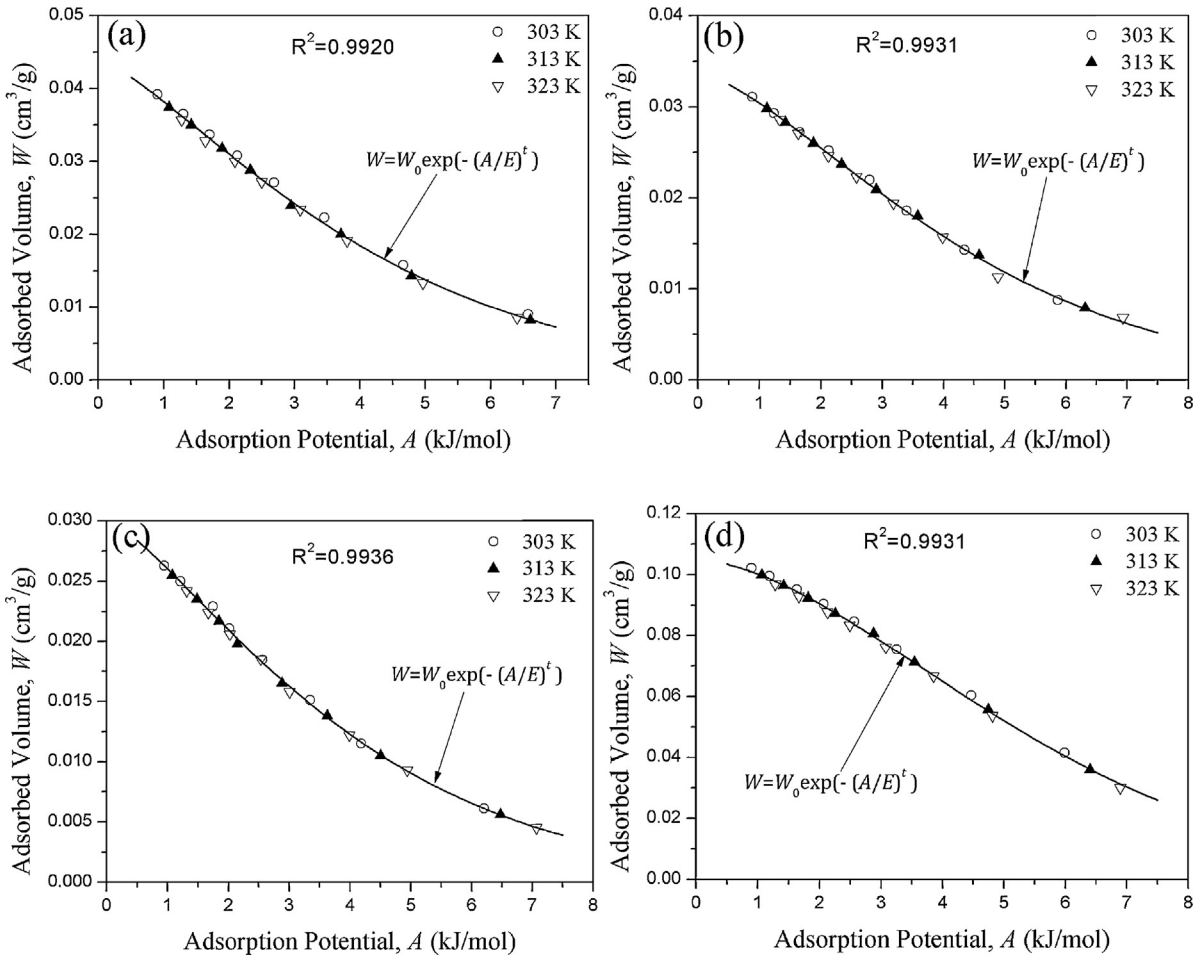

Fig. 3. Characteristic curves for methane on (a) Xingq-1–5#, (b) Qingh-2–3#, (c) Xujd-1#, and (d) Leiy-1#. The p_s was calculated by Dubinin's method.

Eq. (12) when written in terms of amount adsorbed (mmol/g) is [22,31,36]:

$$\frac{n_{\text{absolute}}}{n_0} = \exp\left[-\left(\frac{RT}{E}\ln\frac{p_c\left(T/T_c\right)^k}{p}\right)^t\right] \quad (13)$$

the parameters n_0, E, t, and k are obtained from the regression analysis. The input data for the regression analysis are n_{absolute}, T, and p.

Fig. S4. shows Schwarz curve fits. The adsorption parameters (n_0, E, t, and k) obtained from the regression analysis are listed in Table 4. It can be observed that n_0, E, t, and k are functions of temperature.

Table 4
Adsorption parameters of the D–A model using Schwarz's method to estimate k for calculation pseudo-saturation vapor pressure.

Sample	T	n_0 (mmol/g)	E (kJ/mol)	t	k
Xingq-1–5#	303	0.5967	4.4642	1.2904	1.77
	313	0.5241	4.0845	1.1736	1.23
	323	0.5589	4.0070	1.32	1.77
Qingh-2–3#	303	0.4881	6.0643	1.5661	2.34
	313	0.5176	5.7227	1.6360	2.92
	323	0.3951	4.1856	1.2033	1.12
Xujd-1#	303	0.4044	4.6864	1.3398	1.81
	313	0.3706	4.2399	1.2164	1.42
	323	0.4116	3.7854	1.3485	2.09
Leiy-1#	303	1.5970	7.9912	2.0933	3.51
	313	1.5458	8.4515	2.1454	3.29
	323	1.6213	8.0852	2.4872	4.47

This finding is inconsistent with Schwarz's results [26]. The parameter E in D–A model is characteristic energy which is a measure of the strength of interaction between adsorbate and adsorbent [22]. The adsorption of methane on coal is physical adsorption [46]. The interaction of methane molecules to coal surface is mainly London dispersion forces which are independent of temperature [46]. Consequently, the parameter E should not vary with temperature [22]. The variations of E with temperature could come from the reciprocal influence between the parameters k and t in Eq. (13).

The k values shown in Table 4 can be inserted into Eq. (10) to determine the pseudo- saturation vapor pressure, p_s, which is used to calculate the adsorption potentials, A. And then characteristic curves could be obtained. These characteristic curves are shown in Fig. 4. The solid lines in Fig. 4 represent the characteristic curves calculated by using the regressed adsorption parameters (W_0, E, and t) that are listed in Table S3. The maximum of R^2 is 0.9455 for Xujd-1#, while the minimum of R^2 is 0.6914 for Qingh-2–3#. This indicates that using the Schwarz's method for pseudo-saturation vapor pressure results in data point of characteristic curves being more disperse than the Antoine equation extrapolation and Dubinin's empirical methods.

3.3.4. *Modified Schwarz's method*

It was observed that Schwarz's method did not result in single characteristic curve from Fig. 4. In the present work, we improved the Schwarz's method. In the modified method, the pseudo-saturation vapor pressure is still calculated using the Eq. (10) proposed by Amankwah and Schwarz. However, k which is used to calculate p_s is determined by the following procedure:

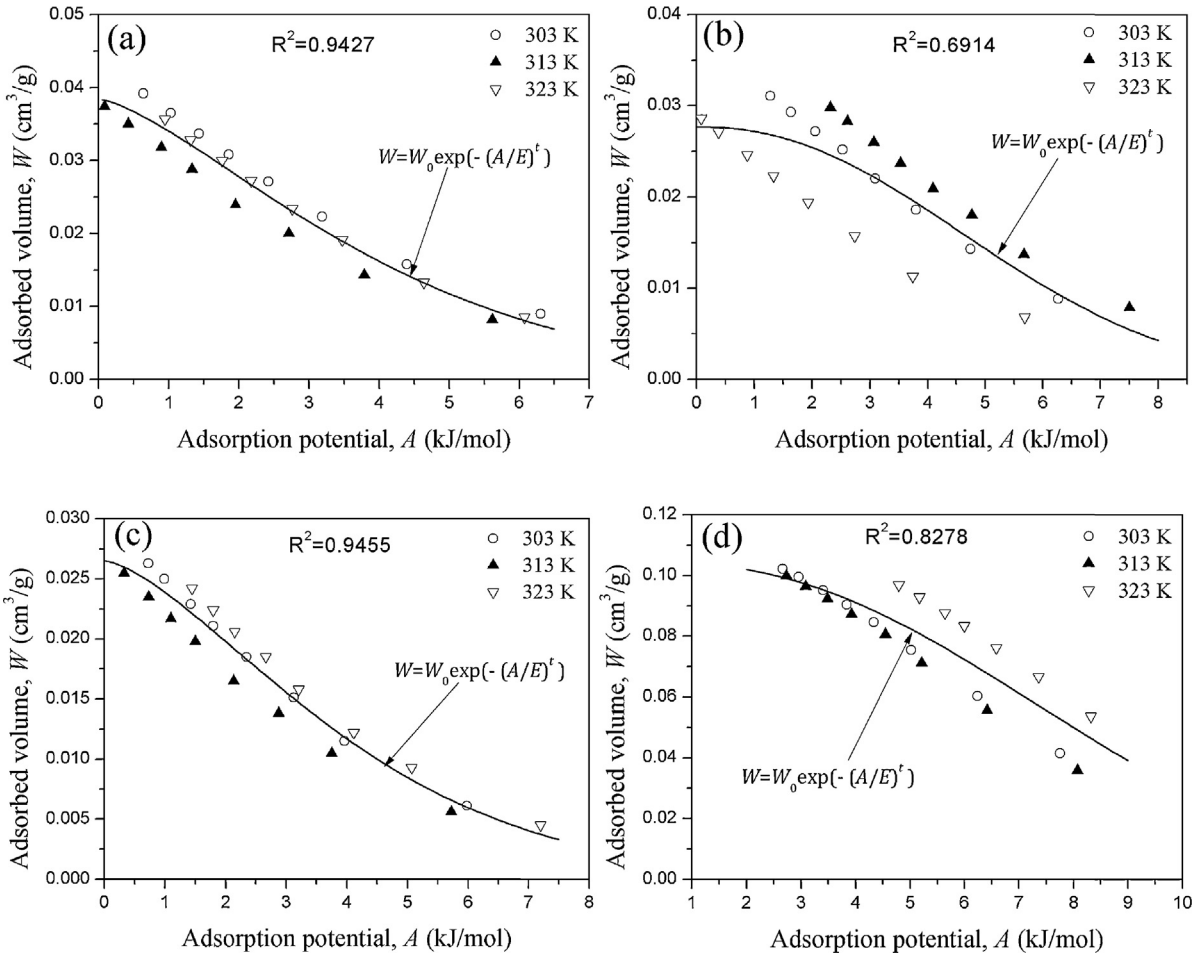

Fig. 4. Characteristic curves for (a) Xingq-1–5#, (b) Qingh-2–3#, (c) Xujd-1#, and (d) Leiy-1#. The p_s was calculated by Schwarz's method.

(1) Let k be equal to 1.6, 2.0, 2.4, . . ., and 4.0 respectively and a series of pseudo-saturation vapor pressure, p_s, which are used to calculate the adsorption potential, A, are obtained;
(2) Plot the relationship between W and A, and the characteristic curves corresponding to different k could be obtained;
(3) Fit the characteristic curves with Eq. (11), and the determination coefficient R^2 could be obtained;
(4) Plot the relationship between R^2 and k, and do regression analysis for the curves. Then, the optimized k which the maximum R^2 corresponds to would be obtained.

Fig. S5 shows the relationship between k and R^2. The data were regressed using the quadratic polynomial. The solid lines in Fig. S5 represent the fitting curves using the regressed parameters (a_0, a_1, and a_2) that are listed in Table S4. Consequently, the optimized value of k is 2.69 for Xingq-1–5#, 2.24 for Qingh-2–3#, 2.26 for Xujd-1#, and 2.7 for Leiy-1#.

Fig. 5 shows the characteristic curves of the samples for which k is taken the optimized value. The solid lines in Fig. 5 are the fitting curves (the black line being Eq. (11) fitting curve and the red line being the cubic polynomial fitting curve respectively). The fitting parameters based on the Eq. (11) are shown in Table 5. The cubic polynomial fitting parameters are shown in Table 6.

As shown in Fig. 5, Table 5 and 6, the modified Schwarz's method to evaluate the pseudo-saturation vapor pressure results in much-improved single characteristic curves for the samples. The value of optimized k is not same for the samples. This is because the adsorbate-adsorbent interaction is not same for the four samples.

Table 5
Regression parameters for the characteristic curves using Eq. (11) as regression equation and p_s being calculated by the modified Schwarz's method.

Sample	W_0 (cm³/g)	E (kJ/mol)	t	R^2
Xingq-1–5#	0.0486	5.0384	1.4490	0.9943
Qingh-2–3#	0.0348	5.0476	1.4789	0.9942
Xujd-1#	0.0311	4.5837	1.3779	0.9946
Leiy-1#	0.1090	6.9336	1.9258	0.9948

The adsorption force field of various adsorbents will uniquely impact adsorbate [26].

3.4. Determination of the characteristic curve form to be utilized

The form of characteristic curve to be utilized is one of the important problems associated with the application of potential theories [11]. The characteristic curve is usually fitted by polynomial [40–42,47]. Although the polynomial fitting is simple, the parameters obtained by regression analysis have no physical

Table 6
Cubic polynomial regression parameters for the characteristic curves (p_s was calculated by the modified Schwarz's method).

Sample	a_0	a_1	a_2	a_3	R^2
Xingq-1–5#	0.0513	−0.0067	-2.4305×10^{-4}	4.9921×10^{-5}	0.9943
Qingh-2–3#	0.0359	−0.0038	-4.8588×10^{-4}	6.1986×10^{-5}	0.9947
Xujd-1#	0.0332	−0.0056	9.7957×10^{-5}	1.8119×10^{-5}	0.9946
Leiy-1#	0.1119	−0.0024	−0.00214	1.4417×10^{-4}	0.9958

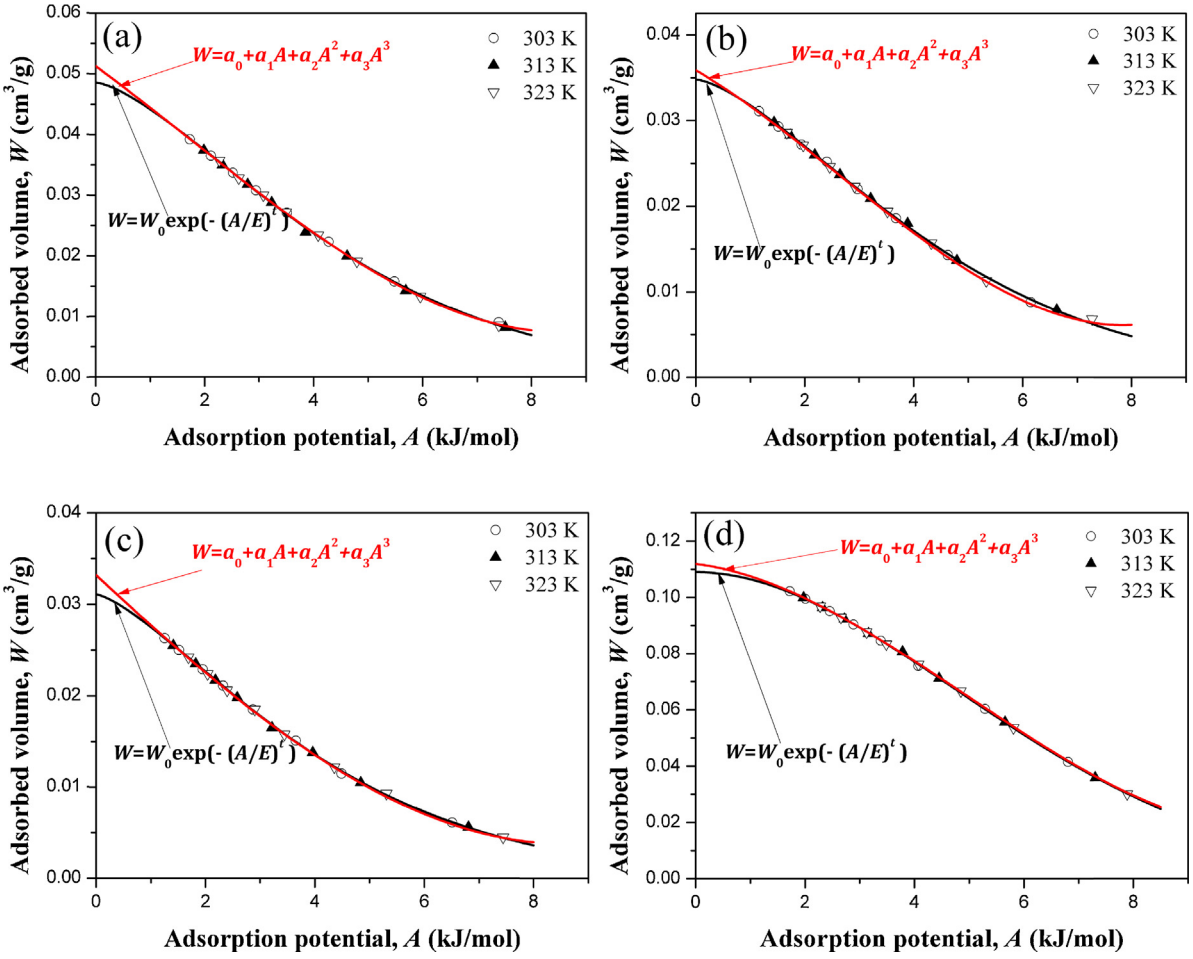

Fig. 5. Characteristic curves for (a) Xingq-1–5#, (b) Qingh-2–3#, (c) Xujd-1#, and (d) Leiy-1#. The p_s was calculated by the modified Schwarz's method.

meaning. As shown in Fig. 5, the different characteristic curve form could result in different W_0 value. The W_0 values obtained from cubic polynomial regression are larger than those obtained from Eq. (11) regression for all coals. To determine the characteristic curve form to be utilized, we use the regression parameters in Table 5 and Table 6, to predict the isotherms at 333 and 343 K, respectively.

When Eq. (11) is used as characteristic curve form, by substituting the regression parameters values reported in Table 5 into Eq. (13), a predictive isotherm equation is obtained for the samples at different temperature which is as follows:

$$n_{\text{absolute}} = n_0 \exp\left[-\left(\frac{\text{RT}}{E}\ln\frac{p_c\left(T/T_c\right)^k}{p}\right)^t\right] \tag{14}$$

where

$$n_0 = \frac{W_0\rho_{\text{adsorbed}}}{M_{\text{CH}_4}} \times 1000 \tag{15}$$

Correspondingly, when cubic polynomial is used as characteristic curve form, by substituting the regression parameters values reported in Table 6 into the following equation, i.e. Eq. (16), a predictive isotherm equation. i.e. Eq. (17) is obtained.

$$\begin{aligned} n_{\text{absolute}} &= \frac{W\rho_{\text{adsorbed}}}{M_{\text{CH}_4}} \times 1000 \\ &= 62.5\rho_{\text{adsorbed}}\left(a_0 + a_1A + a_2A^2 + a_3A^3\right) \end{aligned} \tag{16}$$

$$n_{\text{absolute}} = 62.5\rho_{\text{adsorbed}}\left[a_0 + a_1\frac{\text{RT}\ln\frac{p_c\left(T/T_c\right)^k}{p}}{10^3} + a_2\frac{\left(\text{RT}\ln\frac{p_c\left(T/T_c\right)^k}{p}\right)^2}{10^6} + a_3\frac{\left(\text{RT}\ln\frac{p_c\left(T/T_c\right)^k}{p}\right)^3}{10^9}\right] \tag{17}$$

The value of k in Eqs. (14) and (17) is 2.69 for Xingq-1–5#, 2.24 for Qingh-2–3#, 2.26 for Xujd-1#, and 2.70 for Leiy-1#, respectively (see *3.3.4*). It should be noted that the density of adsorbed phase, ρ_{adsorbed}, is a function of temperature which is calculated by Eq. (2).

Eqs. (14) and (17) allow for the generation of predictive isotherms which can be compared to the experimental data. Plots of isotherms showing a comparison of the experimental and predictive values are shown in Fig. 6. The lines in Fig. 6 refer to the predictive isotherms, while points refer to the laboratory data.

The prediction uncertainty is determined by the mean relative deviation δ:

$$\delta = \sqrt{\frac{1}{N}\sum_{i=1}^{N}\left(\frac{n_{\text{exp,i}} - n_{\text{cal,i}}}{n_{\text{exp,i}}}\right)^2} \tag{18}$$

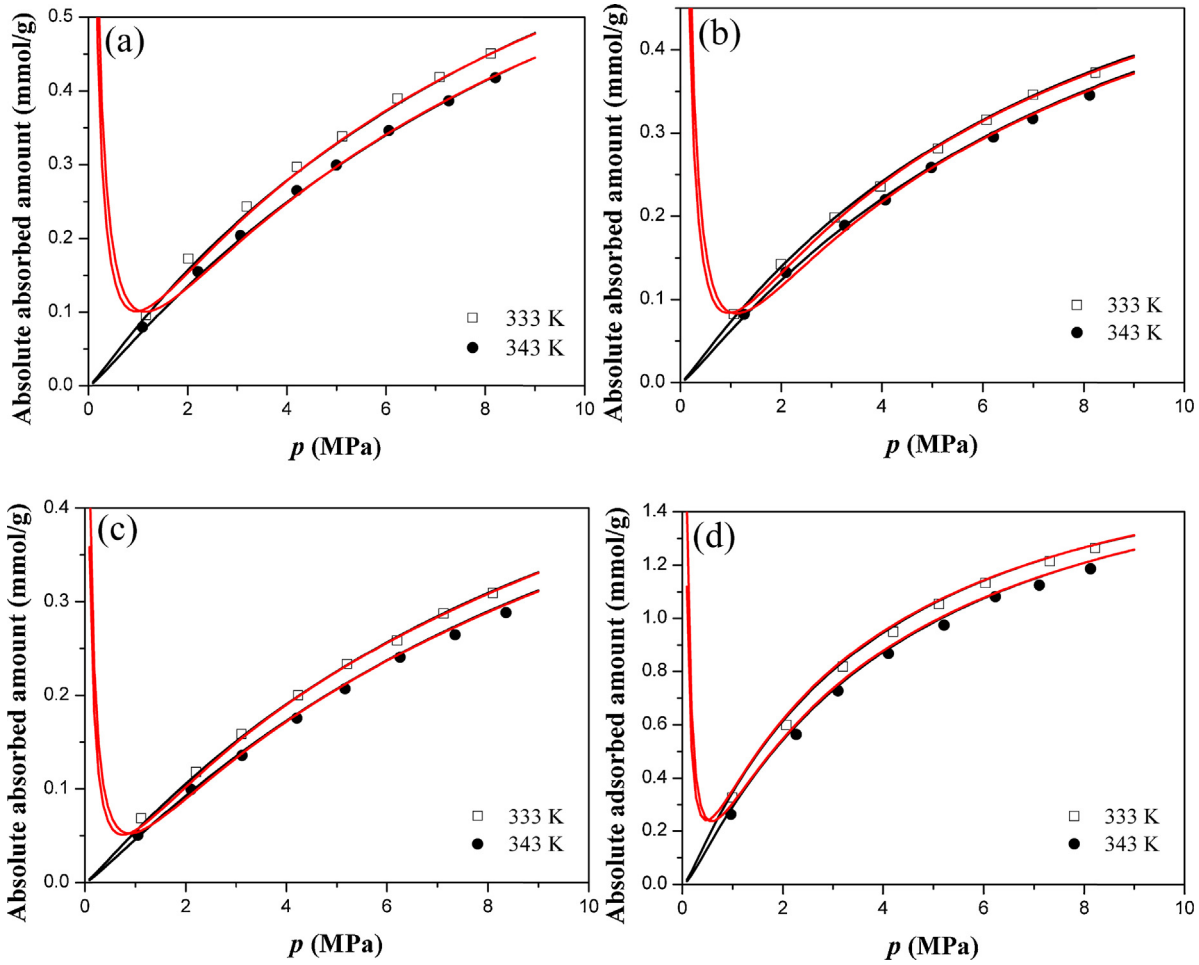

Fig. 6. Experimental vs. predictive isotherms of methane on: (a) Xingq-1–5#, (b) Qingh-2–3#, (c) Xujd-1#, and (d) Leiy-1#. The red lines are predictive isotherms which based on Eq. (17) and the black lines are those which based on Eq. (14).

where N is the number of data points.

The mean relative deviation δ for the two different characteristic curve forms is evaluated and shown in Table 7.

As shown in Fig. 6 and Table 7, the mean relative deviation δ for using Eq. (11) as characteristic curve form is smaller than that for using cubic polynomial as characteristic curve form. In addition, the use of cubic polynomial as the characteristic curve form could result in an abnormal predictive value that the adsorption amount increase with the pressure dropping when the pressure is less than approximately 0.9 MPa for Xingq-1–5# and Xujd-1#, 0.8 MPa for Qingh-2–3#, and 0.5 MPa for Leiy-1#.

Thermodynamics suggests that an adsorption isotherm must exhibit the Henry law behavior when pressure is very low. Unfortunately, the D–A equations do not have the correct Henry law when the pressure is approaching zero. The slope of the D–A adsorption isotherm is zero when the pressure approaches zero when $t > 1$ [22]. However, as shown in Fig. 6, the slope of the D–A adsorption isotherm for using cubic polynomial as characteristic curve form is infinity when the pressure approaches zero. All these indicate that using Eq. (11) as characteristic curve form is more reasonable than using the polynomial.

Table 7
Relative deviation (δ) for predictive isotherms.

Sample	T (K)	Relative deviation, δ (%)	
		Eq. (11)	Cubic polynomial
Xingq-1–5#	333	2.09	3.21
	343	1.83	5.73
Qingh-2–3#	333	1.31	1.82
	343	1.27	2.12
Xujd-1#	333	2.43	6.59
	343	1.65	2.17
Leiy-1#	333	1.79	2.32
	343	2.30	4.29

4. Conclusion

In this work, high pressure (up to 8.3 MPa) adsorption isotherms for methane were obtained at five temperatures for four different rank coals. The Langmuir and D–A equations have been applied to model the adsorption of methane on coals above supercritical temperature.

The temperature dependence of the Langmuir parameter, n_0, indicates that the assumption of an energetically homogeneous surface of adsorption is not strictly true for methane adsorption on coal.

To determine which method to evaluate the pseudo-saturation vapor pressure is most suitable for analyzing the adsorption data above the T_c of methane. The extrapolation of Antoine's equation, Dubinin's method and Schwarz's method for estimating pseudo-saturation vapor pressure were used to test the hypothesis that the data for each adsorption system could be collapsed onto single characteristic curves. It was found that the deviation of characteristic curve data for using Dubinin's method to estimate pseudo-saturation vapor was smaller than those for using the other two methods. However, Dubinin's method do not take into

account uniqueness of the interaction between an adsorbate and a particular adsorbent. Although, Schwarz's method accounts for adsorbate-adsorbate and adsorbate- adsorbent interactions, the adsorption data failed to be reduced to temperature independent plots.

A modified procedure of determining the value of parameter, *k*, in Schwarz's equation, i.e. Eq. (10) was proposed. When this new procedure was applied to analyze the laboratory adsorption data, the adsorption data can be reduced to single temperature invariant characteristic curves for the coals.

The form of characteristic curve could influence D–A equation prediction. Using cubic polynomial as characteristic curve form could result in an abnormal prediction. That is to say the adsorption amount would increase with the pressure dropping. A new form of characteristic curve deduced from D–A equation was proposed. The prediction uncertainty of D–A equation by using this characteristic curve form is less than that for using cubic polynomial as characteristic curve form.

Acknowledgements

This work was supported by the National Basic Research Program of China (973 Program, No. 2011CB201202) and the National Natural Science Foundation of China (20776089).

The authors also thank Jingjie Luo, Wenjing Sun, Ning Wang and Yanyan Feng for their helpful discussions.

Appendix A. Supplementary data

Supplementary data associated with this article can be found, in the online version, at http://dx.doi.org/10.1016/j.colsurfa.2013.12.047.

References

[1] V.K. Gupta, I. Ali, T.A. Saleh, A. Nayak, S. Agarwal, Chemical treatment technologies for waste-water recycling-an overview, RSC Adv. 2 (2012) 6380–6388.
[2] S.A. Grieco, B.V. Ramarao, Removal of TCEP from aqueous solutions by adsorption with zeolites, Colloids Surf. A 434 (2013) 329–338.
[3] V.K. Gupta, S. Agarwal, T.A. Saleh, Chromium removal by combining the magnetic properties of iron oxide with adsorption properties of carbon nanotubes, Water Res. 45 (2011) 2207–2212.
[4] X. Liu, R. Zhu, J. Ma, F. Ge, Y. Xu, Y. Liu, Molecular dynamics simulation study of benzene adsorption to montmorillonite: influence of the hydration status, Colloids Surf. A 434 (2013) 200–206.
[5] A.K. Jain, V.K. Gupta, A. Bhatnagar, Suhas, A comparative study of adsorbents prepared from industrial wastes for removal of dyes, Sep. Sci. Technol. 38 (2003) 463–481.
[6] T.A. Moore, Coalbed methane: A review, Int. J. Coal Geol. 101 (2012) 36–81.
[7] A. Busch, Y. Gensterblum, CBM and CO2-ECBM related sorption processes in coal: a review, Int. J. Coal Geol. 87 (2011) 49–71.
[8] C.R. Clarkson, R.M. Bustin, Variation in micropore capacity and size distribution with composition in bituminous coal of the Western Canadian sedimentary basin: implications for coalbed methane potential, Fuel 75 (1996) 1483–1498.
[9] A. Liu, X. Fu, K. Wang, H. An, G. Wang, Investigation of coalbed methane potential in low-rank coal reservoirs - free and soluble gas contents, Fuel 112 (2013) 14–22.
[10] F. Liu, W. Chu, W. Sun, Y. Xue, Q. Jiang, A DFT study of methane activation on graphite surfaces with vacancy defects, J. Nat. Gas Chem. 21 (2012) 708–712.
[11] C.R. Clarkson, R.M. Bustin, J.H. Levy, Application of the mono/multilayer and adsorption potential theories to coal methane adsorption isotherms at elevated temperature and pressure, Carbon 35 (1997) 1689–1705.
[12] Q. Jiang, W. Chu, W.-J. Sun, F.-S. Liu, Y. Xue, A DFT study of methane adsorption on nitrogen-containing organic heterocycles, Acta Phys. Chim. Sin. 28 (2012) 1101–1106.
[13] M. Bhagiyalakshmi, P. Hemalatha, M. Palanichamy, H.T. Jang, Adsorption, regeneration and interaction of CO_2 with a polythiophene-carbon mesocomposite, Colloids Surf. A 374 (2011) 48–53.
[14] R. Barbero, L. Carnelli, A. Simon, A. Kao, A.D. Monforte, M. Ricco, D. Bianchi, A. Belcher, Engineered yeast for enhanced CO_2 mineralization, Energy Environ. Sci. 6 (2013) 660–674.
[15] H. Jeon, Y.J. Min, S.H. Ahn, S.M. Hong, J.S. Shin, J.H. Kim, K.B. Lee, Graft copolymer templated synthesis of mesoporous MgO/TiO_2 mixed oxide nanoparticles and their CO_2 adsorption capacities, Colloids Surf. A 414 (2012) 75–81.
[16] Y.-S. Jun, D.E. Giammar, C.J. Werth, D.A. Dzombak, Environmental and geochemical aspects of geologic carbon sequestration: a special issue, Environ. Sci. Technol. 47 (2013) 1–2.
[17] E. Santini, E. Guzman, F. Ravera, A. Ciajolo, M. Alfe, L. Liggieri, M. Ferrari, Soot particles at the aqueous interface and effects on foams stability, Colloids Surf. A 413 (2012) 216–223.
[18] M.K. Mondal, H.K. Balsora, P. Varshney, Progress and trends in CO2 capture/separation technologies: a review, Energy 46 (2012) 431–441.
[19] C.M. White, D.H. Smith, K.L. Jones, A.L. Goodman, S.A. Jikich, R.B. LaCount, S.B. DuBose, E. Ozdemir, B.I. Morsi, K.T. Schroeder, Sequestration of carbon dioxide in coal with enhanced coalbed methane recovery: a review, Energy Fuels 19 (2005) 659–724.
[20] S.A. Mohammad, A. Arumugam, R.L. Robinson, K.A.M. Gasem, High-pressure adsorption of pure gases on coals and activated carbon: measurements and modeling, Energy Fuels 26 (2012) 536–548.
[21] H. Xie, H. Zhou, D. Xue, H. Wang, R. Zhang, F. Gao, Research and consideration on deep coal mining and critical mining depth, J.China Coal Soc. 37 (2012) 535–542.
[22] D.D. Do, Adsorption Analysis: Equilibria and Kinetics, Imperial College Press London, London, 1998.
[23] X. Wang, B. Lee, H.T. Chua, Methane desorption and adsorption measurements on activated carbon in 281–343 K and pressures to 1.2 MPa, J. Therm. Anal. Calorim. 110 (2012) 1475–1485.
[24] J. Wen, X. Han, H. Lin, Y. Zheng, W. Chu, A critical study on the adsorption of heterocyclic sulfur and nitrogen compounds by activated carbon: equilibrium, kinetics, and thermodynamics, Chem. Eng. J. 164 (2010) 29–36.
[25] W.S. Loh, A.B. Ismail, B. Xi, K.C. Ng, W.G. Chun, Adsorption isotherms and isosteric enthalpy of adsorption for assorted refrigerants on activated carbons, J. Chem. Eng. Data 57 (2012) 2766–2773.
[26] K.A.G. Amankwah, J.A. Schwarz, A modified approach for estimating pseudo-vapor pressures in the application of the Dubinin–Astakhov equation, Carbon 33 (1995) 1313–1319.
[27] H.J. Kim, Y. Shi, J. He, H.-H. Lee, C.-H. Lee, Adsorption characteristics of CO_2 and CH_4 on dry and wet coal from subcritical to supercritical conditions, Chem. Eng. J. 171 (2011) 45–53.
[28] M.G. Plaza, F. Rubiera, J.J. Pis, C. Pevida, Ammoxidation of carbon materials for CO_2 capture, Appl. Surf. Sci. 256 (2010) 6843–6849.
[29] S. Hao, J. Wen, X. Yu, W. Chu, Effect of the surface oxygen groups on methane adsorption on coals, Appl. Surf. Sci. 264 (2013) 433–442.
[30] J. Xu, W. Chu, S. Luo, Synthesis and characterization of mesoporous V-MCM-41 molecular sieves with good hydrothermal and thermal stability, J. Mol. Catal. A: Chem. 256 (2006) 48–56.
[31] K.A. Rahman, W.S. Loh, H. Yanagi, A. Chakraborty, B.B. Saha, W.G. Chun, K.C. Ng, Experimental adsorption isotherm of methane onto activated carbon at sub- and supercritical temperatures, J. Chem. Eng. Data 55 (2010) 4961–4967.
[32] J. Luo, Y. Liu, C. Jiang, W. Chu, J. Wen, H. Xie, Experimental and modeling study of methane adsorption on activated carbon derived from anthracite, J. Chem. Eng. Data 56 (2011) 4919–4926.
[33] V.M. Gun'ko, Y.V. Zaulychnyy, B.I. Ilkiv, V.I. Zarko, Y.M. Nychiporuk, E.M. Pakhlov, Y.G. Ptushinskii, R. Leboda, J. Skubiszewska-Zieba, Textural and electronic characteristics of mechanochemically activated composites with nanosilica and activated carbon, Appl. Surf. Sci. 258 (2011) 1115–1125.
[34] L. Zhou, Y.P. Zhou, M. Li, P. Chen, Y. Wang, Experimental and modeling study of the adsorption of supercritical methane on a high surface activated carbon, Langmuir 16 (2000) 5955–5959.
[35] B.B. Saha, S. Koyama, I.I. El-Sharkawy, K. Habib, K. Srinivasan, P. Dutta, Evaluation of adsorption parameters and heats of adsorption through desorption measurements, J. Chem. Eng. Data 52 (2007) 2419–2424.
[36] X. Wang, J. French, S. Kandadai, H.T. Chua, Adsorption measurements of methane on activated carbon in the temperature range (281 to 343) K and pressures to 1.2 MPa, J. Chem. Eng. Data 55 (2010) 2700–2706.
[37] D.M. Ruthven, Principles of Adsorption and Adsorption Processes, John Wiley & Sons, New York, 1984.
[38] Y. Zhou, L. Zhou, Study on the adsorption isotherms of supercritical hydrogen on activated carbon, Acta Phys. Chim. Sin. 13 (1997) 119–127.
[39] NIST, Thermophysical properties of fluid systems, http://webbook.nist.gov/chemistry/fluid/
[40] M. Li, A. Gu, X. Lu, R. Wang, Study on methane adsorption above critical temperature by adsorption potential theory, Nat. Gas Chem. Ind. 28 (2003) 28–31.
[41] X. Su, R. Chen, X. Lin, S. Guo, The adsorption characteristic curves of $^{13}CH_4$ and $^{12}CH_4$ on coal and its application, J.China Coal Soc. 32 (2007) 539–543.
[42] Y. Fen, W. Chu, W. Sun, Adsorption characteristics of methane on coal under reservoir temperatures, J.China Coal Soc. 37 (2012) 1488–1492.
[43] R.K. Agarwal, J.A. Schwarz, Analysis of high pressure adsorption of gases on activated carbon by potential theory, Carbon 26 (1988) 873–887.
[44] S. Ozawa, S. Kusumi, Y. Ogino, Physical adsorption of gases at high pressure IV: an improvement of the Dubinin-Astakhov adsorption equation, J. Colloid Interface Sci. 56 (1976) 83–91.
[45] W.S. Loh, K.A. Rahman, A. Chakraborty, B.B. Saha, Y.S. Choo, B.C. Khoo, K.C. Ng, Improved isotherm data for adsorption of methane on activated carbons, J. Chem. Eng. Data 55 (2010) 2840–2847.
[46] B. Nie, S. Duan, The adsorption essence of gas on coal surface, J. Taiyuan Univ. Technol. 29 (1998) 417–421.
[47] X. Su, R. Chen, X. Lin, Y. Song, Application of adsorption potential theory in the fractionation of coalbed gas during the process of adsorption/desorption, Acta Geol. Sin. 82 (2008) 1382–1389.